

Electroweak Phase Transition in Georgi-Machacek Model

Cheng-Wei Chiang^{a,b,c}, Toshifumi Yamada^a

^a *Department of Physics and Center for Mathematics and Theoretical Physics,
National Central University, Chungli, Taiwan 32001, Republic of China*

^b *Institute of Physics, Academia Sinica, Taipei, Taiwan 11529, Republic of China*

^c *Physics Division, National Center for Theoretical Sciences, Hsinchu, Taiwan 30013,
Republic of China*

Abstract

The Georgi-Machacek model extends the standard model Higgs sector by adding two isospin triplet scalar fields and imposing global $SU(2)_R$ symmetry on them. A feature of the model is that the triplets can acquire a large vacuum expectation value without conflicting with the current experimental bound on the ρ parameter. We investigate the electroweak phase transition in the Georgi-Machacek model by evaluating the finite-temperature effective potential of the Higgs sector. The electroweak phase transition can be sufficiently strong in a large parameter space when the triplets acquire a vacuum expectation value of $O(10)$ GeV, opening a possibility to realize successful electroweak baryogenesis.

In spite of the discovery of a Higgs boson at the LHC [1], the structure of the Higgs sector remains largely unexplored. The complete Higgs sector may not be the simplest one containing only one isospin doublet as in the standard model (SM), but may include multiple doublets, a singlet(s) or a triplet(s). One of the motivations to consider such models with an extended Higgs sector comes from electroweak baryogenesis (EWBG) [2], which is the only testable scenario for explaining the observed baryon asymmetry of the Universe. It is well-known that successful EWBG relies on the following two conditions that are not met in the SM:

1. A strong first-order electroweak phase transition that enables decoupling of the sphaleron process in the symmetry broken phase so that created baryon asymmetry is not washed out. More explicitly, the sphaleron process rate in the broken phase should be less than the Hubble parameter at that moment.
2. Large CP-violating phases that enable the creation of sufficient baryon asymmetry through scatterings off the bubble wall separating the broken and symmetric phases.

Of the two conditions, the strong first-order phase transition is directly connected with the field content and structure of the Higgs sector, and hence motivates an extension of the Higgs sector beyond the SM.

Among various models with an extended Higgs sector, the Georgi-Machacek (GM) model with custodial vacuum alignment [3] has unique features that isospin triplet scalars can acquire a large vacuum expectation value (VEV), that this triplet VEV provides an origin for Majorana neutrino mass, and that the model predicts charged Higgs bosons to be tested at colliders [4, 5]. Due to a custodial symmetry that keeps the electroweak ρ parameter unity at tree level, this model allows us to consider the scenario with a large triplet VEV. In this letter, we study how a large triplet VEV of $O(1)$ GeV to $O(10)$ GeV affects the order of electroweak phase transition and whether a sufficiently strong first-order phase transition can be realized in some parameter space of the model. In fact, since the Higgs potential of the GM model contains tree-level triple couplings involving two isospin doublet fields and one triplet or three triplet fields, we expect that a strong first-order phase transition can be achieved *if* the triplets develop a large VEV and are as responsible for electroweak symmetry breaking (EWSB) as the doublet.

In our analysis of electroweak phase transition, we adopt a perturbative approach and evaluate the finite-temperature effective potential at one-loop level [6] for the GM model, from which the strength of phase transition, characterized by v_C/T_C , is evaluated, where T_C and v_C denote respectively the critical temperature and the scalar VEV at the critical temperature. It is well-known that perturbation tends to break down at high temperatures [7], rendering the result of small v_C/T_C less reliable, nevertheless it provides a good order-of-magnitude estimate of the phase transition strength.

This letter is organized as follows. We give quick reviews of the GM model, including its major theoretical and experimental constraints, and of the calculation of the one-loop finite-temperature effective potential. We then conduct a numerical analysis on the strength of electroweak phase transition in various parameter regions of the GM model. In particular, we identify two parameters on which v_C/T_C has significant dependence and find regions with strong first-order phase transition. Discussions of our findings are given toward the end of this letter, followed by a summary.

The Higgs sector of the Georgi-Machacek (GM) model [3] contains one isospin doublet scalar field with hypercharge $Y = 1/2$, denoted by $\phi = (\phi^+, \phi^0)^T = (\phi^+, \frac{1}{\sqrt{2}}(h_\phi + ia_\phi))^T$, one isospin triplet scalar field with $Y = 1$, denoted by $\chi = (\chi^{++}, \chi^+, \chi^0)^T = (\chi^{++}, \chi^+, \frac{1}{\sqrt{2}}(h_\chi + ia_\chi))^T$, and one isospin triplet scalar field with $Y = 0$, denoted by $\xi = (\xi^+, \xi^0, -(\xi^+)^*)^T = (\xi^+, h_\xi, -(\xi^+)^*)^T$. Here h_ϕ, h_χ, h_ξ are CP-even neutral components of the scalar bosons and a_ϕ, a_χ are CP-odd ones. On the Higgs potential, we impose a global $SU(2)_R$ symmetry that is explicitly broken by the SM Yukawa couplings. To make the invariance under the $SU(2)_R$ transformation manifest, we write the Lagrangian in terms of the following $SU(2)_R$ -covariant combinations of fields:

$$\Phi \equiv (\epsilon_2 \phi^*, \phi) = \begin{pmatrix} (\phi^0)^* & \phi^+ \\ -(\phi^+)^* & \phi^0 \end{pmatrix}, \quad (1)$$

$$\Delta \equiv (\epsilon_3 \chi^*, \xi, \chi) = \begin{pmatrix} (\chi^0)^* & \xi^+ & \chi^{++} \\ -(\chi^+)^* & \xi^0 & \chi^+ \\ (\chi^{++})^* & -(\xi^+)^* & \chi^0 \end{pmatrix}, \quad (2)$$

where

$$\epsilon_2 = \begin{pmatrix} 0 & 1 \\ -1 & 0 \end{pmatrix}, \quad \epsilon_3 = \begin{pmatrix} 0 & 0 & 1 \\ 0 & -1 & 0 \\ 1 & 0 & 0 \end{pmatrix}. \quad (3)$$

Under the $SU(2)_L \times SU(2)_R$ symmetry, Φ and Δ transform as $\Phi \rightarrow U_{2L} \Phi U_{2R}^\dagger$ and $\Delta \rightarrow U_{3L} \Delta U_{3R}^\dagger$, respectively, where U_2 is the two-dimensional representation of $SU(2)$ group and U_3 is the three-dimensional one. The Higgs sector Lagrangian is then expressed as

$$\mathcal{L} = \frac{1}{2} \text{tr}[(D^\mu \Phi)^\dagger D_\mu \Phi] + \frac{1}{2} \text{tr}[(D^\mu \Delta)^\dagger D_\mu \Delta] - V_{tree}(\Phi, \Delta) - (\text{Yukawa terms}). \quad (4)$$

where D_μ denotes the covariant derivative for Φ or Δ . Explicit expressions of the Yukawa terms, particularly those responsible for neutrino mass, can be found in Ref. [4], and are omitted here

for simplicity. The tree-level Higgs potential $V_{tree}(\Phi, \Delta)$ is given by

$$\begin{aligned}
V_{tree}(\Phi, \Delta) &= \frac{1}{2}m_1^2 \text{tr}[\Phi^\dagger\Phi] + \frac{1}{2}m_2^2 \text{tr}[\Delta^\dagger\Delta] \\
&+ \lambda_1 (\text{tr}[\Phi^\dagger\Phi])^2 + \lambda_2 (\text{tr}[\Delta^\dagger\Delta])^2 + \lambda_3 \text{tr} \left[(\Delta^\dagger\Delta)^2 \right] + \lambda_4 \text{tr}[\Phi^\dagger\Phi]\text{tr}[\Delta^\dagger\Delta] \\
&+ \lambda_5 \sum_{a,b=1,2,3} \text{tr} \left[\Phi^\dagger \frac{\sigma^a}{2} \Phi \frac{\sigma^b}{2} \right] \text{tr}[\Delta^\dagger T^a \Delta T^b] \\
&+ \mu_1 \sum_{a,b=1,2,3} \text{tr} \left[\Phi^\dagger \frac{\sigma^a}{2} \Phi \frac{\sigma^b}{2} \right] (P^\dagger \Delta P)_{ab} + \mu_2 \sum_{a,b=1,2,3} \text{tr}[\Delta^\dagger T^a \Delta T^b] (P^\dagger \Delta P)_{ab} , \quad (5)
\end{aligned}$$

where σ 's are the Pauli matrices,

$$\begin{aligned}
T^1 &= \frac{1}{\sqrt{2}} \begin{pmatrix} 0 & 1 & 0 \\ 1 & 0 & 1 \\ 0 & 1 & 0 \end{pmatrix} , \quad T^2 = \frac{1}{\sqrt{2}} \begin{pmatrix} 0 & -i & 0 \\ i & 0 & -i \\ 0 & i & 0 \end{pmatrix} , \quad T^3 = \begin{pmatrix} 1 & 0 & 0 \\ 0 & 0 & 0 \\ 0 & 0 & -1 \end{pmatrix} , \\
\text{and } P &= \frac{1}{\sqrt{2}} \begin{pmatrix} -1 & i & 0 \\ 0 & 0 & 1 \\ 1 & i & 0 \end{pmatrix} .
\end{aligned}$$

We take $m_1^2 < 0$ as in the SM and $m_2^2 > 0$. In this case, the EWSB caused by the VEV of the doublet field will induce the triplet field to develop a VEV as well through the μ_1 term. Finally, we assume no CP violation in the newly introduced terms of the Lagrangian.

The EWSB vacuum at tree level is derived by solving the following tadpole conditions:

$$\frac{\partial V(\Phi, \Delta)}{\partial h_\phi} = \frac{\partial V(\Phi, \Delta)}{\partial h_\chi} = \frac{\partial V(\Phi, \Delta)}{\partial h_\xi} = 0 , \quad (6)$$

with fields other than $h_\phi, h_\chi,$ and h_ξ being zero. From Eq. (6), we choose the solution with the relation $h_\chi = \sqrt{2}h_\xi$, by which the EWSB vacuum maintains a diagonal $SU(2)_{L+R}$ or $SU(2)_V$ symmetry. Writing the VEV's of h_ϕ, h_χ, h_ξ as $\langle h_\phi \rangle = v_1, \langle h_\chi \rangle = \sqrt{2}v_2, \langle h_\xi \rangle = v_2$, respectively, we have $|\langle h_\phi \rangle|^2 + 2|\langle h_\chi \rangle|^2 + 4|\langle h_\xi \rangle|^2 = v^2 \simeq (246 \text{ GeV})^2$. Here we define $\tan \theta_H$ as the VEV ratio, $\tan \theta_H \equiv 2\sqrt{2}v_2/v_1$. When $v_1, v_2 \neq 0$, one can use Eq. (6) to rewrite m_1^2, m_2^2 in terms of the VEV's of h_ϕ, h_χ, h_ξ and other parameters in the Higgs potential as

$$\begin{aligned}
m_1^2 &= -4\lambda_1 v_1^2 - 6\lambda_4 v_2^2 - 3\lambda_5 v_2^2 - \frac{3}{2}\mu_1 v_2 , \\
m_2^2 &= -12\lambda_2 v_2^2 - 4\lambda_3 v_2^2 - 2\lambda_4 v_1^2 - \lambda_5 v_1^2 - \mu_1 \frac{v_1^2}{4v_2} - 6\mu_2 v_2 . \quad (7)
\end{aligned}$$

We can derive the field-dependent mass matrices of the scalar bosons from Eq. (5) to be used in the evaluation of the finite-temperature effective potential. After substituting $h_\phi = v_1, h_\chi = \sqrt{2}h_\xi = \sqrt{2}v_2$ and Eq. (7) and diagonalizing the mass matrices, one finds three massless

Nambu-Goldstone modes that eventually become the longitudinal components of the W and Z bosons. Under the classification of $SU(2)_V$ symmetry, the other massive states are grouped into a 5-plet $H_5 = (H_5^{++}, H_5^+, H_5^0, H_5^-, H_5^{--})^T$, a 3-plet $H_3 = (H_3^+, H_3^0, H_3^-)^T$, and two singlets H_1^0 and H_1^0 . Among these particles, only the 3-plet is CP-odd while the others are CP-even. The two singlets generally mix to produce physical states denoted by H and h , where the latter is used to denote the recently discovered SM-like Higgs boson. As a result of the custodial symmetry, the components in each of the above-mentioned multiplets are degenerate in mass. Mass splittings of the order of a few hundred MeV due to electromagnetic breaking are expected within each representation, but can be safely ignored for our study. As a reference, we give their mass eigenvalues at the EWSB vacuum, with the help of Eq. (7), as:

$$m_{H_5}^2 = 8\lambda_3 v_2^2 - \frac{3}{2}\lambda_5 v_1^2 - \frac{\mu_1 v_1^2}{4v_2} - 12\mu_2 v_2, \quad (8)$$

$$m_{H_3}^2 = -\left(\frac{\lambda_5}{2} + \frac{\mu_1}{4v_2}\right)v^2, \quad (9)$$

$$m_{H,h}^2 = 4\lambda_1 v_1^2 + 4(3\lambda_2 + \lambda_3)v_2^2 - \frac{\mu_1 v_1^2}{8v_2} + 3\mu_2 v_2 \pm \left\{ \left[4\lambda_1 v_1^2 + 4(3\lambda_2 + \lambda_3)v_2^2 - \frac{\mu_1 v_1^2}{8v_2} + 3\mu_2 v_2 \right]^2 - 4v_1^2 v_2^2 [16\lambda_1(3\lambda_2 + \lambda_3) - 3(2\lambda_4 + \lambda_5)^2] + 2\lambda_1 \frac{\mu_1 v_1^4}{v_2} + \frac{3}{4}\mu_1^2 v_1^2 + 6v_1^2 v_2(2\lambda_4 \mu_1 + \lambda_5 \mu_1 - 8\lambda_1 \mu_2) \right\}^{1/2}. \quad (10)$$

We comment on various limits of the GM model. The triplet VEV v_2 vanishes when one sets $\mu_1 = 0$, as long as $m_2^2 > 0$, $\lambda_4 > 0$ and $\lambda_5 > 0$ are assumed. In other words, the triplet VEV is induced by the doublet VEV through the μ_1 term. The GM model becomes SM-like, *i.e.*, the extra Higgs bosons H_3, H_5, H are decoupled and the triplet VEV vanishes, when we take the limits of $\mu_1, v_2 \rightarrow 0$ with $\mu_1/v_2 \rightarrow \infty$. A detailed discussion about the decoupling limit of the GM model is recently discussed in Ref. [9].

Now we enumerate the theoretical and experimental constraints on the GM model that will be incorporated in our parameter search for viable electroweak phase transition. First, we consider the stability of the Higgs potential at large field values. To avoid any runaway direction in the Higgs potential, Refs. [8, 4] have found the following conditions on the coupling constants λ_i :

$$\begin{aligned} \lambda_1 > 0, \quad \lambda_2 + \lambda_3 > 0, \quad \lambda_2 + \frac{1}{2}\lambda_3 > 0, \quad -|\lambda_4| + 2\sqrt{\lambda_1(\lambda_2 + \lambda_3)} > 0, \\ \lambda_4 - \frac{1}{4}|\lambda_5| + \sqrt{2\lambda_1(2\lambda_2 + \lambda_3)} > 0. \end{aligned} \quad (11)$$

For perturbative calculations to be valid, we further impose the unitarity bound from the S -wave amplitudes for elastic scatterings of two scalar boson states. The strongest bound as found in Ref. [10] is:

$$|12\lambda_1 + 22\lambda_2 + 14\lambda_3 \pm \sqrt{(12\lambda_1 - 22\lambda_2 - 14\lambda_3)^2 + 144\lambda_4^2}| < 16\pi . \quad (12)$$

In subsequent analyses, we will restrict ourselves to the parameter space with $\tan\theta_H < 0.5$ ($v_2 < 39$ GeV). This choice is made so that the constraints from both the $Z \rightarrow b\bar{b}$ decay [4] and the electroweak S parameter are satisfied in the entire region [5].

At the one-loop level, the finite-temperature effective potential of the Higgs sector is given by [6]

$$V^1(\varphi; T) = V_B(\varphi) + V_0^1(\varphi, \mu_R) + \frac{T^4}{2\pi^2} \left[\sum_{i \in \text{Bosons}} n_i I_B(m_i(\varphi)^2/T^2) + \sum_{i \in \text{Fermions}} n_i I_F(m_j(\varphi)^2/T^2) \right], \quad (13)$$

where T denotes the temperature, φ collectively denotes the values of the fields, $m_i(\varphi)$ denotes the field-dependent mass of mass eigenstate i , and n_i counts its degrees of freedom. $V_B(\varphi)$ is the same function as Eq. (5) with the parameters $m_1^2, m_2^2, \lambda_1, \lambda_2, \lambda_3, \lambda_4, \lambda_5, \mu_1, \mu_2$ being replaced by the corresponding bare parameters that should be fixed by nine renormalization conditions at zero temperature. $V_0^1(\varphi, \mu_R)$ is the one-loop effective potential at zero temperature renormalized at the scale μ_R , which is given by [11]

$$V_0^1(\varphi, \mu_R) = \frac{1}{64\pi^2} \left[\sum_{i \in \text{Bosons}} n_i (m_i^2(\varphi))^2 \left\{ \log\left(\frac{m_i^2(\varphi)}{\mu_R^2}\right) - C_i \right\} - \sum_{i \in \text{Fermions}} n_i (m_i^2(\varphi))^2 \left\{ \log\left(\frac{m_i^2(\varphi)}{\mu_R^2}\right) - C_i \right\} \right] \quad (14)$$

where μ_R is the renormalization scale and C_i 's are constants that depend on the renormalization scheme. The functions I_B, I_F are defined as

$$I_B(a^2) = \int_0^\infty dx x^2 \log \left[1 - \exp(-\sqrt{x^2 + a^2}) \right], \quad (15)$$

$$I_F(a^2) = \int_0^\infty dx x^2 \log \left[1 + \exp(-\sqrt{x^2 + a^2}) \right], \quad (16)$$

respectively, and interpolating functions are employed in numerical evaluations.

We adopt the Landau gauge in our calculations. We include in ‘Bosons’ of Eq. (13) the W and Z bosons, the (field-dependent) mass eigenstates of Higgs bosons and the would-be

Nambu-Goldstone modes. In ‘Fermions’, we include only the SM top quark neglecting the other SM matter fields.

We evaluate the strength of electroweak phase transition characterized by v_C/T_C , the ratio of the Higgs VEV at the critical temperature and the critical temperature T_C , in a wide range of parameter space in the GM model. We choose $\tan\theta_H$, λ_1 , λ_2 , λ_3 , λ_4 , λ_5 , μ_1 and μ_2 as the independent parameters. We then fix the value of λ_1 by the requirement that the mass of the lightest CP-even boson be 126 GeV, the mass of the currently observed Higgs boson.

Two of the nine renormalization conditions require that the zero-temperature one-loop effective potential, $V_B + V_0^1$, have a minimum at $h_\phi = v \cos\theta_H$, $h_\chi = \frac{1}{2}v \sin\theta_H$. The relation $h_\xi = \frac{1}{2\sqrt{2}}v \sin\theta_H$ automatically follows from these conditions due to $SU(2)_R$ symmetry of the potential. The other seven renormalization conditions require the matching of components of the scalar boson mass matrices and three-point coupling constants evaluated from the tree-level potential Eq. (5) and those evaluated from the zero-temperature one-loop effective potential, $V_B + V_0^1$.

We note in passing that, since the field-dependent mass eigenstates include the would-be Nambu-Goldstone modes that become massless for $h_\phi = v \cos\theta_H$, $h_\chi = \frac{1}{2}v \sin\theta_H$, $h_\xi = \frac{1}{2\sqrt{2}}v \sin\theta_H$, some of the renormalization conditions apparently contain $\log 0$ singularity. In fact, terms containing $\log 0$ singularity vanish in dimensional regularization if they originate from the integral $\int d^D p / (2\pi)^D p^\alpha$ with $\alpha \neq -2$ and $D = 4 - 2\epsilon$. The integral $\int d^D p / (2\pi)^D p^{-2}$ gives $\Gamma(\epsilon)/(4\pi)^D$, which is subtracted in the $\overline{\text{MS}}$ scheme leaving no finite terms [12].

After determining the bare parameters by the renormalization conditions, we numerically evaluate the critical temperature T_C and the VEV of the fields at T_C , defined as $v_C \equiv \sqrt{|\langle h_\phi \rangle_{T_C}|^2 + 2|\langle h_\chi \rangle_{T_C}|^2 + 4|\langle h_\xi \rangle_{T_C}|^2}$, using the finite-temperature one-loop effective potential in Eq. (13). In the course of numerical analysis, we exclude unphysical parameter regions where

- the mass spectrum contains a negative squared mass;
- the potential is unbounded from below for large field values, namely, the vacuum stability condition Eq. (11) is not fulfilled;
- the perturbative unitarity condition Eq. (12) is violated; or
- the electroweak symmetry breaking vacuum (with $\langle h_\phi \rangle = v_1$, $\langle h_\chi \rangle = \sqrt{2}v_2$ and $\langle h_\xi \rangle = v_2$) is not the absolute minimum of the zero-temperature one-loop effective potential.

In our study, we have found that the strength of phase transition has a stronger dependence on λ_4 and $\tan\theta_H$ than on the other parameters in the Higgs potential. In the following, we

illustrate this by making contour plots of v_C/T_C on the plane of $(\lambda_4, \tan\theta_H)$ while holding $\lambda_2, \lambda_3, \lambda_5, \mu_1$ and μ_2 fixed. In Figs. 1 to 3, we pick three sets of parameters and focus on the region of $0 < \lambda_4 < 0.8$ and $0.1 < \tan\theta_H < 0.5$ to show the viability of strong first-order phase transition. The condition on the strength of electroweak phase transition for successful baryogenesis is expressed as [2]

$$v_C/T_C \gtrsim \zeta, \quad (17)$$

where ζ is determined by the sphaleron decoupling condition and is usually about 1. In each plot, we enclose the region of $1 < v_C/T_C < 2$ by the thick black dashed curves and that of $v_C/T_C > 2$ by the thick black solid curves. We have found that, in the parameter space of interest, the vacuum stability condition Eq. (11) provides the strongest constraint among those listed above, and hence we mark the regions where this condition is violated by the purple areas in the plots.

In Fig. 1, we fix $\lambda_{2,3,5} = 0.4$ and take $\mu_1 = \mu_2 = -100$ GeV in the left plot and -300 GeV in the right plot. In Fig. 2, we fix $\lambda_{2,3,5} = 0.6$ with the same choices of μ_1, μ_2 for the left and right plots as in Fig. 1. In Fig. 3, we fix $\lambda_2 = 0.7, \lambda_{3,5} = 0.6$, which are almost maximally allowed values, and μ_1, μ_2 are the same as in Fig. 1. If we take larger values for $\lambda_{2,3,5}$ (*e.g.*, ~ 0.7), then most of the parameter space is excluded due to the violation of perturbative unitarity, Eq. (12). From Figs. 1, 2 and 3, we observe that strong first-order phase transition, $v_C/T_C \gtrsim 1$, can be achieved generally in the region with large $\tan\theta_H$ and large λ_4 . This is particularly apparent in the plots with $\mu_1 = \mu_2 = -300$ GeV. For the selected sets of parameters, the realization of $v_C/T_C \gtrsim 1$ requires $\tan\theta_H \gtrsim 0.15$, corresponding to $v_2 \gtrsim 13$ GeV. This is consistent with our expectation that a large triplet VEV helps enhancing the strength of phase transition because it gives rise to a sizeable tree-level triple Higgs boson coupling. We also find that the realization of strong first-order phase transition, since the lower bound on $\tan\theta_H$ required for $v_C/T_C \gtrsim 1$ becomes smaller as the values of λ_4 and/or $\lambda_{2,3,5}$ increase. This is in accordance with the general argument that large quartic couplings for the Higgs boson and extra bosons enhance the value of v_C/T_C . In our case, radiative corrections from the additional bosonic fields to the finite-temperature effective potential are proportional to $\lambda_{2,3,4,5}$ and induce an effective triple Higgs coupling to trigger the first-order phase transition. However, if $-\mu_1 = -\mu_2 = 100$ GeV, v_C/T_C is below 1 for even larger values of $\tan\theta_H$ and λ_4 .

The dependence of v_C/T_C on $\tan\theta_H$ can be understood as follows. Let us consider the

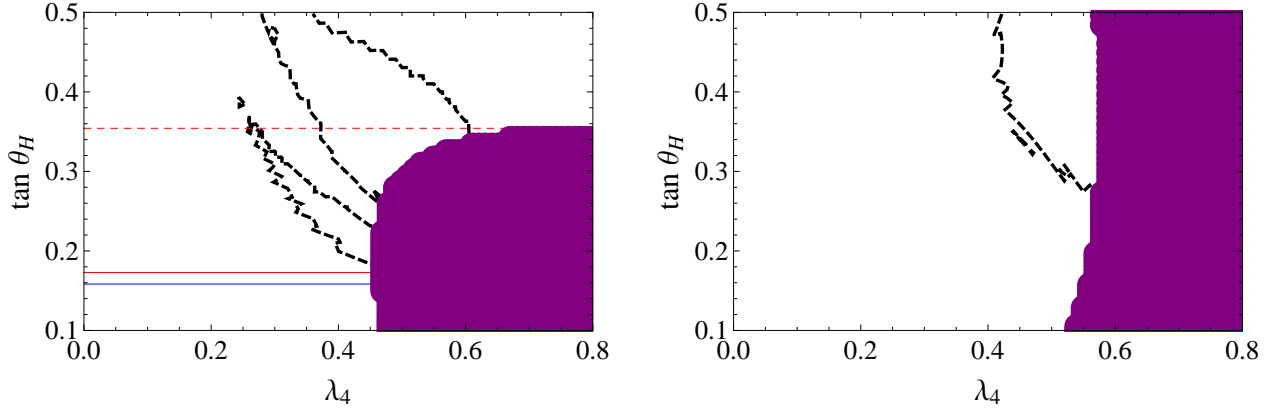


Figure 1: Contours of v_C/T_C on the λ_4 - $\tan\theta_H$ plane. In both plots, we fix $\lambda_{2,3,5} = 0.4$. λ_1 is determined so that the lightest CP-even Higgs boson has the mass of 126 GeV. The region filled by purple is unphysical due to vacuum instability. The region surrounded by the thick black dashed curves corresponds to $1 < v_C/T_C < 2$, and that outside to $v_C/T_C < 1$. In the left plot, we take $\mu_1 = \mu_2 = -100$ GeV. $140 \text{ GeV} < m_{H_3} < 200 \text{ GeV}$ above the red dashed line and $200 \text{ GeV} < m_{H_3} < 300 \text{ GeV}$ between the red dashed and red solid lines. $200 \text{ GeV} < m_{H_5} < 300 \text{ GeV}$ above the blue solid line. In the right plot, we take $\mu_1 = \mu_2 = -300$ GeV. Here $m_{H_{3,5}} > 300 \text{ GeV}$ in the entire physically allowed region.

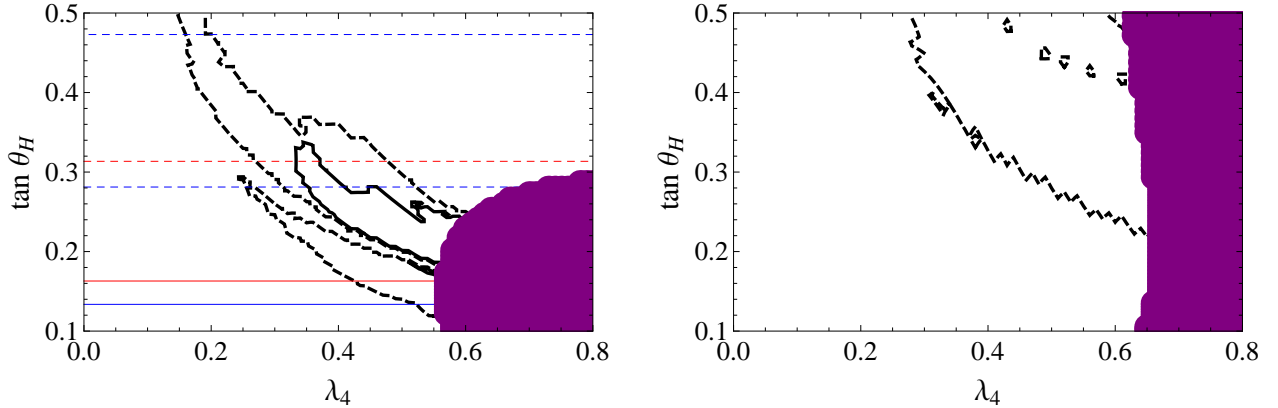


Figure 2: Same as Fig. 1, but here we fix $\lambda_{2,3,5} = 0.6$. The region surrounded by the thick black solid curves corresponds to $2 < v_C/T_C < 3$. In the left plot, $140 \text{ GeV} < m_{H_3} < 200 \text{ GeV}$ above the red dashed line and $200 \text{ GeV} < m_{H_3} < 300 \text{ GeV}$ between the red dashed and red solid lines. $140 \text{ GeV} < m_{H_5} < 200 \text{ GeV}$ between the blue dashed lines and $200 \text{ GeV} < m_{H_5} < 300 \text{ GeV}$ between the lower blue dashed and blue solid lines, and above the upper blue dashed line. In the right plot, both m_{H_3} and m_{H_5} are above 300 GeV in the entire physically allowed region.

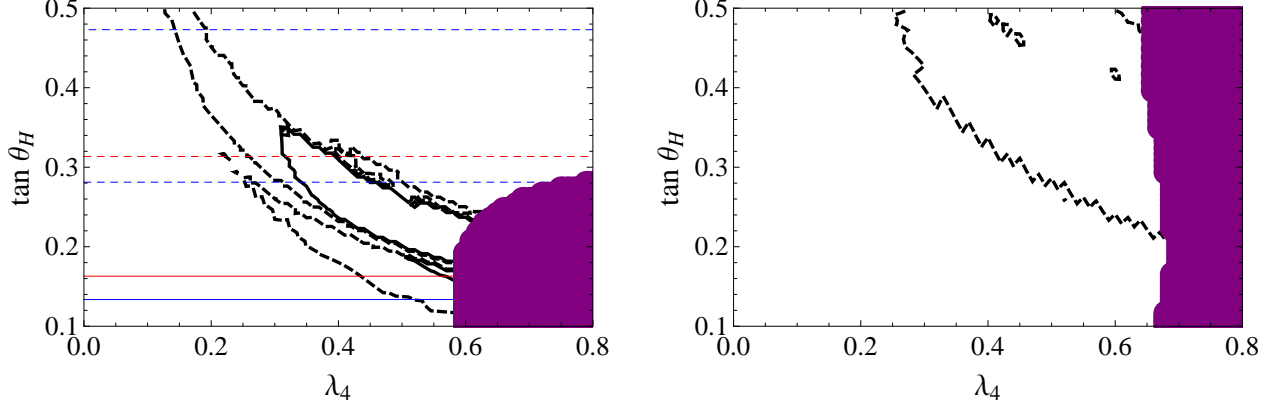


Figure 3: Same as Fig. 1, but here we fix $\lambda_2 = 0.7$, $\lambda_{3,5} = 0.6$. Note that the domain of $2 < v_C/T_C < 3$ is slightly wider compared to the case with $\lambda_{2,3,5} = 0.6$.

following orthogonal transformation on the CP-even neutral fields in the GM model,

$$\begin{pmatrix} h_1 \\ h_2 \\ h_3 \end{pmatrix} = A \begin{pmatrix} 0 & \frac{1}{A} \sqrt{\frac{1}{3}} & -\frac{1}{A} \sqrt{\frac{2}{3}} \\ \sqrt{3} \sin \theta_H & -\frac{4}{\sqrt{3}} \cos \theta_H & -2\sqrt{\frac{2}{3}} \cos \theta_H \\ 2\sqrt{2} \cos \theta_H & \sqrt{2} \sin \theta_H & \sin \theta_H \end{pmatrix} \begin{pmatrix} h_\phi \\ h_\chi \\ h_\xi \end{pmatrix} \quad (18)$$

where $A \equiv 1/\sqrt{8 \cos^2 \theta_H + 3 \sin^2 \theta_H}$. Among the fields on the left-hand side, only h_3 develops a VEV at zero temperature and hence plays a key role in the electroweak phase transition. The field h_3 has a tree-level triple coupling that originates from the terms proportional to μ_1 or μ_2 in the Higgs potential (the last line of Eq. (5)), given by

$$V_{tree}(\Phi, \Delta) \supset 6A^3 (\mu_1 \cos^2 \theta_H \sin \theta_H + \mu_2 \sin^3 \theta_H) h_3^3, \quad (19)$$

independent of λ_i 's. As $\tan \theta_H$ increases (but below 0.5), the first term on the right hand side of Eq. (19) is enhanced and gives a significant contribution to the triple coupling of h_3 . Such a large triple coupling generally enhances the order of phase transition when μ_1 is negative. However, large $\tan \theta_H$ also induces a large quartic coupling of h_3 as

$$V_{tree}(\Phi, \Delta) \supset A^4 (32\lambda_1 \cos^4 \theta_H + 9\lambda_2 \sin^4 \theta_H + 3\lambda_3 \sin^4 \theta_H + 24\lambda_4 \cos^2 \theta_H \sin^2 \theta_H + 12\lambda_5 \cos^2 \theta_H \sin^2 \theta_H) h_3^4. \quad (20)$$

The term proportional to λ_4 , in particular, has a sizeable contribution if $\tan \theta_H$ and λ_4 are both large. Such a large quartic coupling of h_3 in turn suppresses the order of phase transition, competing with the enhancement of the order of phase transition by the triple coupling. Therefore, we observe that v_C/T_C has the tendency of first increasing with $\tan \theta_H$ and then decreasing for even larger $\tan \theta_H$ when the other parameters are fixed.

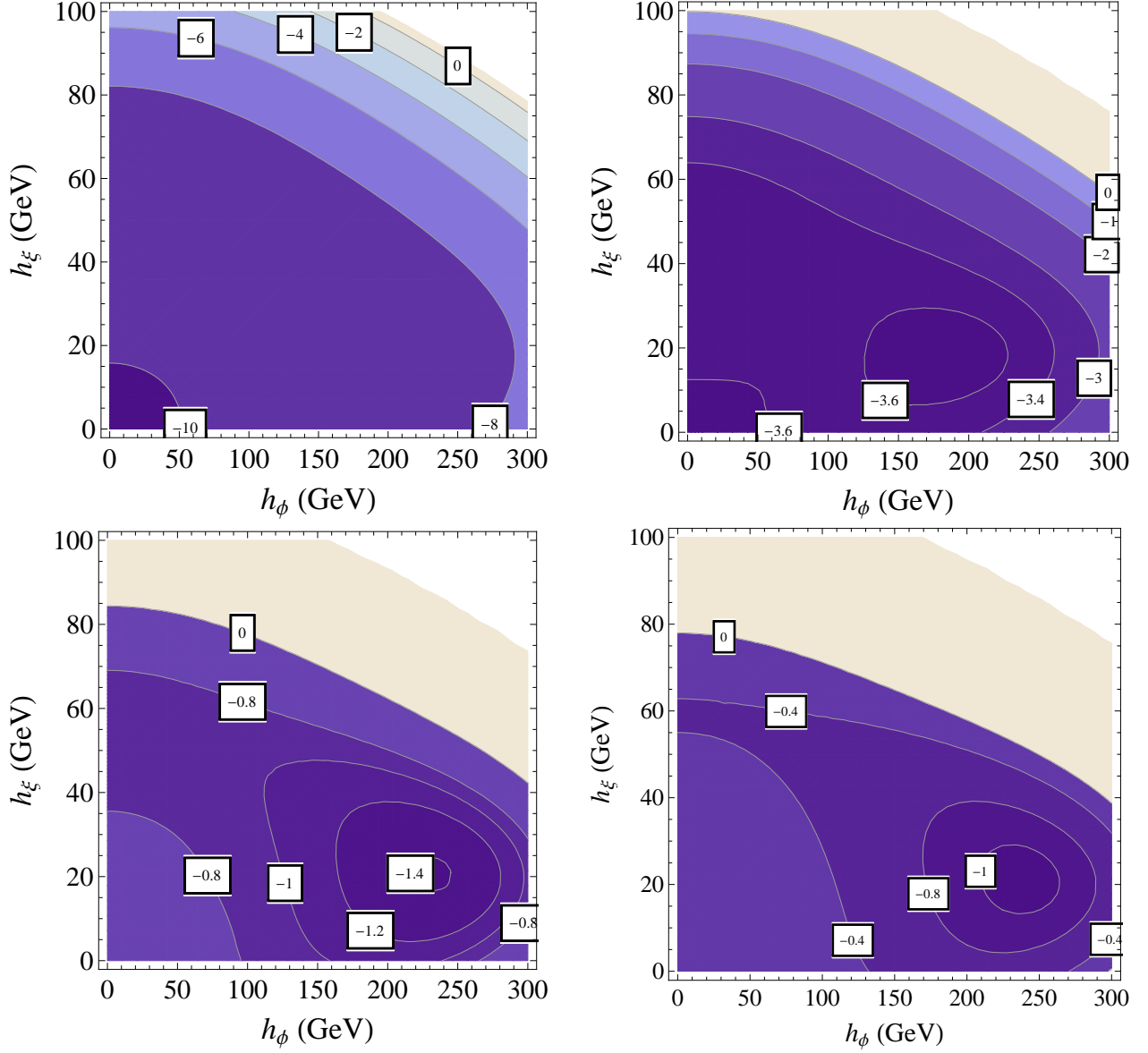


Figure 4: Contour plots of the value of the Higgs potential at $T = 120$ GeV (upper left), $T = 92.5$ GeV $\simeq T_C$ (upper right), $T = 60$ GeV (lower left), and $T = 0$ GeV (lower right), at the parameter point of $\lambda_{2,3,5} = 0.6$, $\lambda_4 = 0.4$, $\mu_1 = \mu_2 = -100$ GeV and $\tan \theta_H = 0.25$. The numbers labeled on the contours are in units of $(100 \text{ GeV})^4$.

To examine how such strong first-order electroweak phase transition occurs in the regions with $v_C/T_C > 2$, we take as one example the parameter choice of $\lambda_{2,3,5} = 0.6$, $\lambda_4 = 0.4$, $\mu_1 = \mu_2 = -100$ GeV and $\tan \theta_H = 0.25$, which sits right inside the region surrounded by the solid curve in Fig. 2. Fig. 4 presents contour plots of the Higgs potential on the plane of (h_ϕ, h_ξ) with $h_\chi = \sqrt{2}h_\xi$ assumed, at $T = 120$ GeV, $T = 92.5$ GeV $\simeq T_C$, $T = 60$ GeV, $T = 0$ GeV, where T_C denotes the critical temperature for this parameter choice. The number on each contour gives the value of the Higgs potential in units of $(100 \text{ GeV})^4$. Here we observe that, as temperature approaches the critical temperature from above, a local minimum other than the origin develops and eventually becomes the absolute minimum below the critical temperature.

Collider phenomenology of the new Higgs bosons in the GM model at LHC had been extensively classified and analyzed in Ref. [4]. In particular, specific channels and kinematic cuts were proposed to search for such bosons. Here we compute the masses of the $SU(2)_V$ 3-plet and 5-plet, m_3 and m_5 , and superimpose their contours in Figs. 1 to 3. As apparent from Eqs. (8) and (9), m_3 and m_5 do not have any dependence on λ_4 . It turns out that both m_3 and m_5 are above 300 GeV in the entire physical region of each right plot of Figs. 1 to 3, where $\mu_1 = \mu_2 = -300$ GeV. On the other hand, m_3 and m_5 can go below 300 GeV in the left plots, where $\mu_1 = \mu_2 = -100$ GeV. Note that since m_3 and m_5 are both above 140 GeV in the entire physically allowed domains in these figures, the mass spectra considered here safely evade the LEP bound on charged scalars.

In summary, we have found the regions on the λ_4 - $\tan \theta_H$ plane that grant strong first-order phase transition after fixing the other five parameters. If new sources of CP violation beyond the SM Yukawa couplings are provided, successful electroweak baryogenesis will be possible in these regions. However, since all the coupling constants in the GM model are real if $SU(2)_R$ symmetry is imposed, and since terms that explicitly break $SU(2)_R$ symmetry are constrained by the experimental value of the ρ parameter, it is necessary to further extend the GM model to incorporate additional CP-violating phases. We have discovered that strong first-order phase transition characterized by $v_C/T_C \gtrsim 1$ is generally realized for large values of $\tan \theta_H$ and/or large values of λ_4 in the GM model. The strength is further enhanced for larger quartic couplings, subject to the constraints of perturbative unitarity and Higgs potential stability. For the selected parameter sets, the minimum of $\tan \theta_H$ with which strong first-order phase transition is viable is about 0.15, corresponding to the triplet VEV $v_2 \simeq 13$ GeV.

Acknowledgments

C.-W. C. thanks the hospitality of the Theoretical Particle Physics Group at Nagoya University during his visit and where part of this work was carried out. T. Y. thanks Dr. Kei Yagyu for useful discussions of the Georgi-Machacek model. This research was supported in part by the National Science Council of R.O.C. under Grant Nos. NSC-100-2628-M-008-003-MY4 and NSC-102-2811-M-008-019.

References

- [1] ATLAS Collaboration, *Phys. Lett. B* **716** (2012) 1 [arXiv:1207.7214 [hep-ex]]; CMS Collaboration, *Phys. Lett. B* **716** (2012) 30 [arXiv:1207.7235 [hep-ex]]; *JHEP* **06** (2013) 081 [arXiv:1303.4571 [hep-ex]].
- [2] V. A. Kuzmin, V. A. Rubakov and M. E. Shaposhnikov, *Phys. Lett. B* **155** (1985) 36; A. G. Cohen, D. B. Kaplan and A. E. Nelson, *Nucl. Phys. B* **349** (1991) 727; *Ann. Rev. Nucl. Part. Sci.* **43** (1993) 27; M. Quiros, *Helv. Phys. Acta* **67** (1994) 451; V. A. Rubakov and M. E. Shaposhnikov, *Usp. Fiz. Nauk* **166** (1996) 493 [*Phys. Usp.* **39** (1996) 461].
- [3] H. Georgi and M. Machacek, *Nucl. Phys. B* **262** (1985) 463.
- [4] C.-W. Chiang and K. Yagyu, *JHEP* **1301** (2013) 026 [arXiv:1211.2658 [hep-ph]].
- [5] C.-W. Chiang, A.-L. Kuo and K. Yagyu, arXiv:1307.7526 [hep-ph].
- [6] L. Dolan and R. Jackiw, *Phys. Rev. D* **9** (1974) 3320.
- [7] R. R. Parwani, *Phys. Rev. D* **45** (1992) 4695 [Erratum-*ibid.* *D* **48** (1993) 5965] [hep-ph/9204216].
- [8] A. Arhrib, R. Benbrik, M. Chabab, G. Moulhaka, M. C. Peyranere, L. Rahili and J. Ramadan, *Phys. Rev. D* **84** (2011) 095005 [arXiv:1105.1925 [hep-ph]].
- [9] K. Hartling, K. Kumar and H. E. Logan, arXiv:1404.2640 [hep-ph].
- [10] M. Aoki and S. Kanemura, *Phys. Rev. D* **77** (2008) 095009 [arXiv:0712.4053 [hep-ph]].
- [11] S. R. Coleman and E. J. Weinberg, *Phys. Rev. D* **7** (1973) 1888.
- [12] D. M. Capper and G. Leibbrandt, *J. Math. Phys.* **15**, 82 (1974).